Can. J. Remote Sensing, Vol. 33, No. 6, pp. 519–533, 2007

Mapping piping plover (*Charadrius melodus melodus*) habitat in coastal areas using airborne lidar data

R. Goodale, C. Hopkinson, D. Colville, and D. Amirault-Langlais

Abstract. Coastal estuaries and beach habitat are some of the most important and productive ecosystems in Atlantic Canada. These sensitive areas are crucial for hundreds of land and marine species. Mapping and monitoring coastal habitat is important for the protection of species such as the endangered piping plover (*Charadrius melodus melodus*). Light detection and ranging (lidar) elevation and intensity data have been used together to successfully classify land-cover types. This study explores the use of elevation, texture, slope, and intensity to classify coastal habitat. Lidar data were collected over a barrier beach and estuary on the South Shore of Nova Scotia. Ground validation and training sites were collected using a real-time kinematic global positioning system. Unsupervised, supervised, and logical filter classifications were compared for separability of various beach and intertidal habitats. Coastal land classes similar in elevation, texture, and slope, such as mudflats, sand beaches, and salt marshes, relied heavily on intensity data for separation. Tidal saturation of these areas produced similar intensity returns, resulting in poor separation between classes. Logical filters applied to the lidar data improved the classification of coastal habitat compared to standard unsupervised and supervised classifications. Additional logical filters were used to isolate important nesting and feeding habitat for piping plover. Results of this study suggest that lidar can effectively be used for classifying coastal habitat if tidal and seasonal factors are taken into consideration.

Résumé. Les estuaires côtiers et les habitats de plage sont parmi les écosystèmes les plus importants et productifs dans la région atlantique au Canada. Ces zones sensibles sont cruciales pour des centaines d'espèces terrestres et marines. La cartographie et le suivi des habitats côtiers sont essentiels pour la protection des espèces comme le pluvier siffleur (*Charadrius melodus melodus*), une espèce menacée. Des données d'altitude et d'intensité lidar (« light detection and ranging ») ont été utilisées conjointement avec succès pour la classification des types de couvert. La présente étude explore l'utilisation de l'altitude, de la texture, de la pente et de l'intensité pour la classification des habitats côtiers. Les données lidar ont été acquises au-dessus d'un cordon littoral et d'un estuaire sur la côte sud de la Nouvelle-Écosse. Les sites de validation et d'entraînement au sol ont été collectés en utilisant un système de positionnement global cinématique en temps réel. Les résultats des classifications non dirigée, dirigée et par filtre logique ont été comparés dans le contexte de la séparabilité des divers habitats de plage ou intertidaux. La séparation des classes semblables de couvert côtier en termes d'altitude, de texture et de pente telles que les vasières, les plages sablonneuses et les marais salants reposait fortement sur les données d'intensité. La saturation par la marée de ces zones a produit des retours d'intensité semblables résultant en une faible séparation entre les classes. L'application de filtres logiques aux données lidar a permis d'améliorer la classification des habitats côtiers comparativement aux classifications standards non dirigée et dirigée. Des filtres logiques additionnels ont été utilisés pour isoler les habitats importants de nidification et d'alimentation pour le pluvier siffleur. Les résultats de cette étude suggèrent que les données lidar peuvent être utilisées efficacement pour la classification des habitats côtiers si les facteurs tidaux et saisonniers sont pris en considération.
[Traduit par la Rédaction]

Introduction

Coastal habitats are typically comprised of intertidal and beach–dune zones in Atlantic Canada. Intertidal zones consist of estuaries, mudflats, sandflats, and salt-marsh habitats (Rangeley and Singh, 2000). Beach–dune zones commonly encompass sand, gravel, or cobble beaches and sand-dune systems (Department of Fisheries and Oceans Canada, 1996). Intertidal and coastal beaches are important nesting and feeding areas for a variety of shorebirds in Eastern Canada. Certain coastal areas have been identified as critical habitat by the Canadian Wildlife Service for species such as the endangered

Received 4 May 2007. Accepted 22 October 2007. Published on the *Canadian Journal of Remote Sensing* Web site at http://pubs.nrc-cnrc.gc.ca/cjrs on 15 February 2008.

R. Goodale,[1] C. Hopkinson, and D. Colville. Applied Geomatics Research Group (AGRG), Centre of Geographic Sciences, NSCC Annapolis Valley Campus, 50 Elliott Road, R.R. 1, Lawrencetown, NS B0S 1M0, Canada.

D. Amirault-Langlais. Canadian Wildlife Service, Environment Canada, PO Box 6227, Sackville, NB E4L 1G6, Canada.

[1]Corresponding author (e-mail: ryangoodale@hotmail.com).

© 2007 CASI

piping plover (*Charadrius melodus melodus*). Intertidal estuaries, ephemeral ponds, sand and gravel beaches, and shorelines of salt marshes and sand, mud, and algal flats are essential feeding areas for the piping plover and other migratory shorebirds (US Fish and Wildlife Service, 1996; Environment Canada, 2006; Haig and Elliott-Smith, 2004; Morrison et al., 1995). Classification and delineation of these areas as critical habitat and preservation of coastal habitat are important for the recovery of the piping plover (Environment Canada, 2006).

Airborne light detection and ranging (lidar) systems have been used in many coastal applications from coastal flood risk assessments (Webster et al., 2005) to shoreline change (Gibeaut et al., 2001). The unique feature of these systems is the collection of high-resolution elevation data over large areas at decimetre levels of accuracy for the production of detailed surface models. Topographic features along coastal beaches and estuaries can be accurately mapped with lidar systems (Baltsavias, 1999; French, 2003). These areas are usually devoid of thick overstory vegetation, allowing for optimal ground reflectance from laser pulses, which results in detailed elevation models showing subtle changes in terrain. More recently, lidar intensity data coupled with elevation data have been used for land-cover classifications (Brennan and Webster, 2006; Beasy et al., 2005; Charaniya et al., 2004; Song et al., 2002). Intensity is an index of the maximum amount of energy, in the near-infrared portion of the electromagnetic spectrum, reflected by the returned laser signal (Wehr and Lohr, 1999) and is controlled by the peak power and footprint area of the emitted pulse (Hopkinson, 2007). Intensity values can be gridded to produce an image comparable to that of grey-scale digital photography. This study examines the use of lidar intensity and elevation-derived data products to classify coastal beach and estuary habitat. In addition, the use of a logical filter classification is compared to standard classification methods.

Study area

Coastal beaches and intertidal sand, mudflats, and algal flats along the South Shore of Nova Scotia are used extensively by shorebirds for nesting, feeding, and migration habitat during the spring, summer, and fall months (Morrison et al., 1995). Johnston's Pond Beach is located 3 km southwest of the community of Port L'Hebert along the South Shore of Nova Scotia (see **Figure 1**). The area consists of an 800 m long coastal barrier beach with an inlet channel leading into an estuary with expansive mudflats and salt marsh. On the coastal side of the beach is a raised cobble barrier beach with flat sandy areas within the intertidal zone. On the lagoon side of the beach is an area of sand, mixed sand, and cobble along with small dunes with patches of marram grass (*Ammophila* sp.). The sandy area leads into mudflats, salt marsh, and thickly vegetated, small stabilized dune systems. A maximum of nine adult pairs of piping plover were observed on the beach in 1983. Over the last few years, two pairs of piping plover have consistently nested on Johnston's Pond Beach (Boates et al., 1994).

Johnston's Pond Beach is of particular interest owing to its variety of beach and intertidal zone substrates. Furthermore, this area has been identified as critical habitat for piping plover because of the long history of nesting at this site (Boates et al., 1994; Environment Canada, 2006). Johnston's Pond also provides nesting habitat for other avian species, such as the common tern (*Sterna hirundo*) and willet (*Catoptrophorus semipalmatus*), and feeding habitat for a variety of shorebirds during migration, such as the semipalmated plover (*Charadrius semipalmatus*), semipalmated sandpiper (*Calidris pusilla*), and dunlin (*Calidris alpina*). In addition, the small beach size allowed for detailed ground measurements and validation for comparison with the lidar data.

Methodology

Field validation

Using a Leica SR530 RTK global positioning system (GPS), points were collected for validating lidar elevations and image classifications. The horizontal and vertical positional accuracies of the RTK system are documented as 10 + 1 ppm (root mean square (rms)) and 20 + 1 ppm (rms), respectively (Leica Geosystems AG, 1999). To validate lidar coordinate elevations, over 400 GPS points were collected along the length and width of the runway that the survey aircraft took off from. A further 40 GPS points were collected around the edge of a nearby large flat building roof to validate horizontal point coordinate locations. In addition, 78 random points were collected around the Johnston's Pond area to validate the lidar land-cover classifications. Points were also collected in transects across land covers and as polygons to delineate various beach features to be used as training sites for the coastal habitat classifications. Transect locations were determined based on areas that best represented the majority of substrate and vegetation types found in the area. Polygons covered homogeneous features representing substrate and vegetation types. Areas of interest for coastal habitat training sites were as follows: (*i*) sand, (*ii*) cobble (1–20 cm diameter) – bedrock, (*iii*) mixed (>10% sand mixed with cobble (i.e., pebbles, stones, rocks)), (*iv*) mudflat–sandflat (organic–sand mixtures and saturated sand), (*v*) vegetated mudflat (mudflat covered in vegetation (i.e., grasses, salt-marsh vegetation)), (*vi*) patchy dune vegetation (<75% cover), (*vii*) thick dune vegetation (≥75% cover), and (*viii*) trees and shrubs.

Sand, mixed, and patchy vegetation habitat classes are key nesting areas for piping plover on the South Shore of Nova Scotia (Flemming et al., 1992). Conversely, thick vegetation, trees and shrubs, and cobble areas are unlikely to be used for nesting (Flemming et al., 1992). Thick vegetation and shrubs provide shelter for approaching predators, and therefore open and sparsely vegetated areas are preferred for viewing approaching threats (Burger, 1987). Sand and pebble substrates are required for producing nest scrapes, which are shallow depressions used for nesting. Pure sand, pebbles, and sand mixed with cobbles are substrates that provide varying degrees

© 2007 CASI

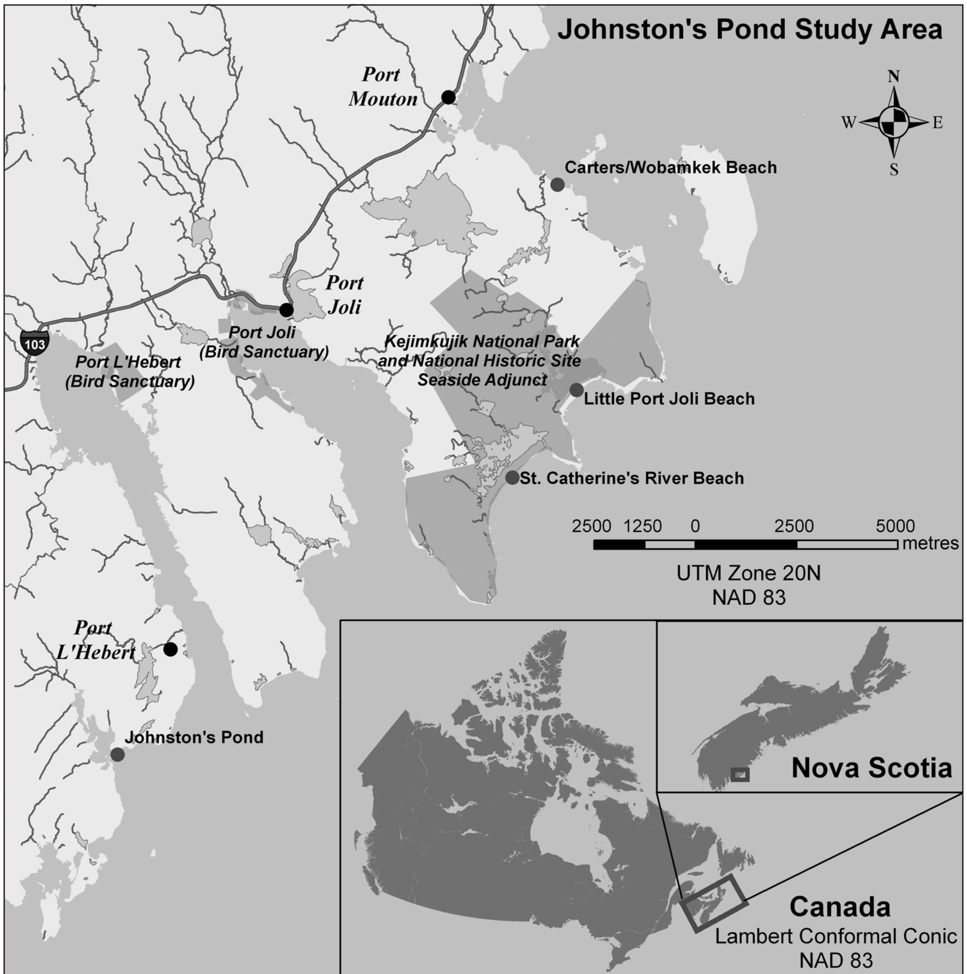

Figure 1. South shore of Nova Scotia, Canada, showing the location of Johnston's Pond Beach.

of camouflage for the eggs which is important for protection from predators (Flemming et al., 1992; Haig and Elliott-Smith, 2004). Open sand, mudflats, or sandflats immediately adjacent to nesting grounds are critical feeding areas for juvenile piping plover before they can fly (Environment Canada, 2006), whereas densely vegetated mudflats are more difficult to access.

Lidar processes

The lidar system used was an Optech Airborne Laser Terrain Mapper (ALTM) 3100 system from the Applied Geomatics Research Group (AGRG), Centre of Geographic Sciences (COGS), installed on a Cessna Skymaster survey aircraft. The data were collected on 4 October 2005 from an airborne platform altitude of 2000 m above the ground. A pulse repetition frequency (PRF) of 50 kHz and a scan frequency of 24 Hz resulted in an approximate resolution of 0.6 m point spacing at ground level. The lidar data were processed at the AGRG, and the raw laser points were classified into ground, non-ground, and all-hits using a TerraScan (version 005.005) module running on the Bentley Microstation software platform (V8 2004 edition).

To validate the lidar *X–Y–Z* coordinate data, three sets of six lines were flown over the runway used for the survey flight and a nearby large building. Elevation (*Z*) was tested by flying six lines perpendicular to the runway and collecting full swaths of lidar data that could be directly compared with the GPS validation points. Validation of lidar coordinates in the along-track flight direction (*X*) was performed by flying perpendicular to the building edge and collecting six profiles (0° scan angle) of points over the building edge break line. Validation of lidar coordinates in the cross-track flight direction (*Y*) was performed by flying along the building edge and scanning a swath of points left and right across the building edge break line. The comparison of lidar coordinates and GPS validation data was performed using Auto Calibrator (version 1.3.0.27), a proprietary software package provided by Optech, the ALTM manufacturer. For the elevation validation, all lidar points within a 0.5 m radius of a GPS point were compared and a summary of the statistics for each flight line was provided. For the horizontal *X* and *Y* positional validation, Auto Calibrator filters the lidar point data to identify the break-line position at which the lidar scan or profile encounters the building edge. The lidar break lines are then compared with the

© 2007 CASI

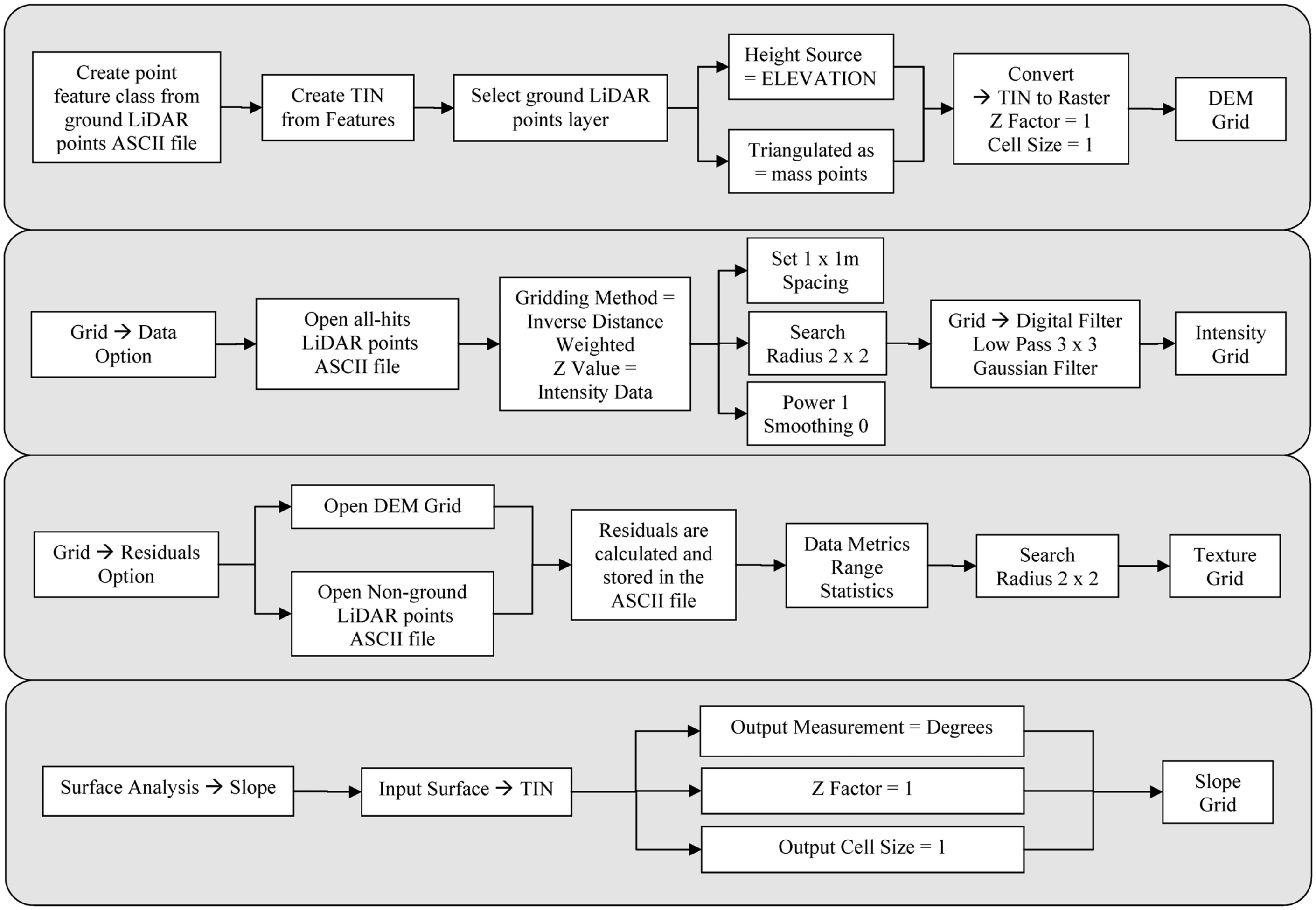

Figure 2. Workflows for creating DEM, intensity, texture, and slope rasters. Input parameters are shown for creating DEM and slope rasters using ArcGIS 3D Analyst. Inputs for creating intensity and texture rasters were applied using Surfer.

surveyed building edge, and the horizontal offsets calculated and summarized per flight line.

Classification of lidar imagery

Four parameters were used in the classification of beach habitat on Johnston's Pond Beach: intensity, elevation, texture, and slope. Intensity coupled with elevation data has been shown to be effective for land-cover classifications (Wehr and Lohr, 1999; Song et al., 2002; Charaniya et al., 2004; Brennan and Webster, 2006). In addition, Beasy et al. (2005) successfully completed a classification of shoreline features on a beach along the Bay of Fundy, Nova Scotia, using intensity and surface texture attributes that were derived from the lidar elevation data. The ALTM sensor used in this study can read up to four simultaneous returns from the laser signal. Usually, in the case of multiple signal returns from a single emitted pulse, the first return is reflected from above-ground structures such as treetops, for example, and the last return reflects from or near to ground level. Last returns are usually filtered to remove non-ground returns, and the remaining ground level returns are used to derive digital elevation models (DEMs), whereas first and intermediate returns from above the ground surface are useful in determining the vertical profile of objects such as forest canopies or buildings (Burtch, 2002; Wehr and Lohr, 1999). Texture is a measure of variation in heights from the DEM and non-ground laser returns. By subtracting the intersecting DEM raster elevation values from the non-ground laser return points, the residuals can be gridded to show landscape texture. Furthermore, the slope of the terrain can be derived from the DEM.

Using the software package Surfer (version 8, Golden Software Inc.), an intensity raster was created from the "all hits" ALTM intensity return values using an inverse distance weighted (IDW) interpolation method. A DEM was created using ArcGIS 3D Analyst (version 9.1, Environmental Systems Research Institute Inc.) by interpolating the ground laser returns using a linear interpolated triangulated irregular network (TIN), which was then converted to a raster. By subtracting the DEM from the raw non-ground laser pulse returns, the height above ground was determined for each laser pulse. Using the Surfer data metrics range interpolation option, height ranges within a 2 m search radius were converted to a raster to show landscape texture.

© 2007 CASI

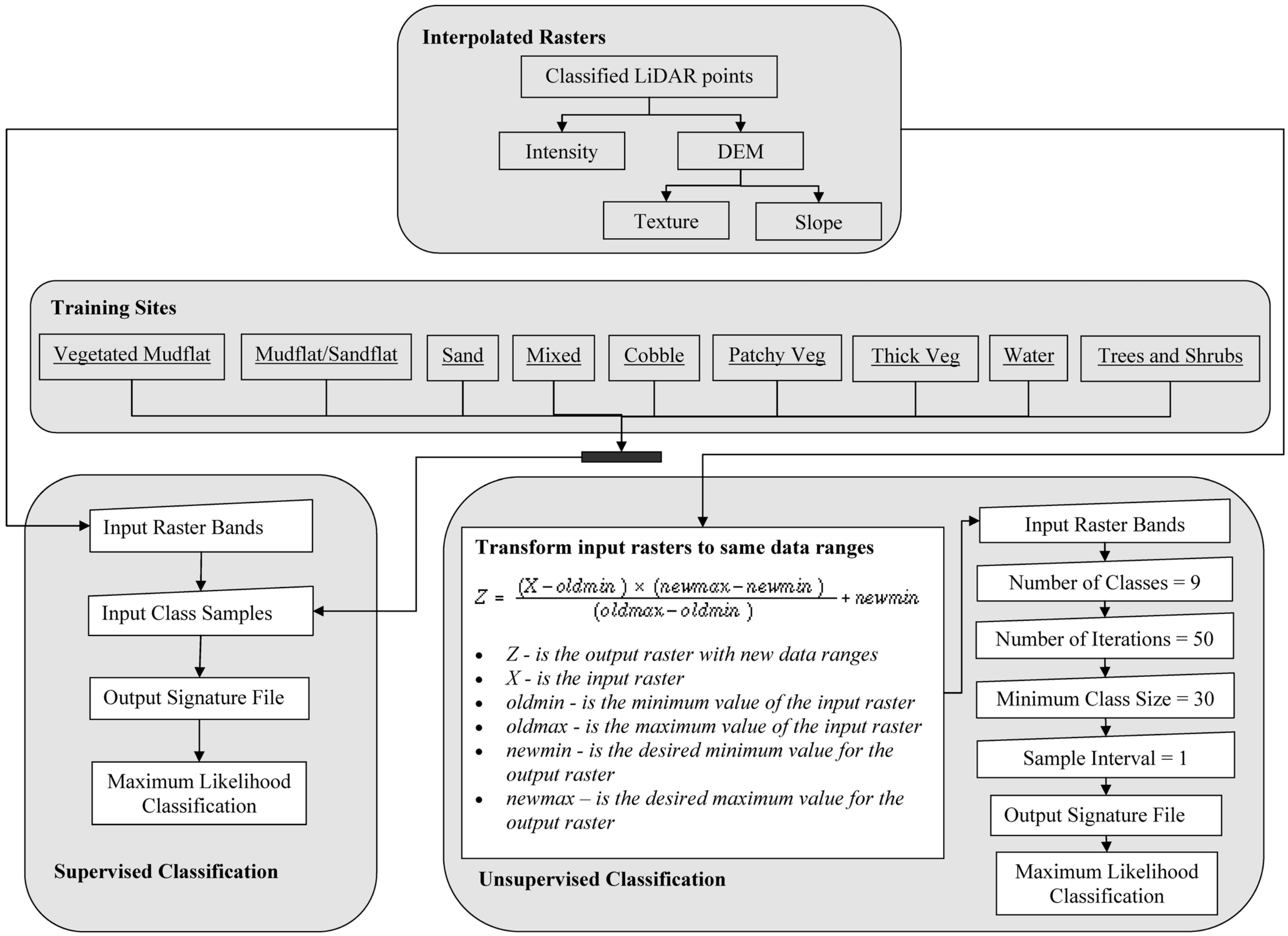

Figure 3. Illustration of the supervised and unsupervised classification workflows. Nine training sites were used as signatures to classify the four input rasters using a supervised classification method. The unsupervised classification method used an isoclustering algorithm to create the class signatures. For optimal results, the four rasters were transformed to the same data ranges. The newly transformed data ranges were grouped into nine class signatures after 50 iterations of the clustering algorithm. Each pixel was sampled and grouped into a minimum class size of 30 pixels. Both the supervised and unsupervised classifications methods used a maximum likelihood classification to classify the pixels into one of the classes represented in the signature files.

Lastly, a slope raster was created from the DEM using the 3D Analyst slope option (see **Figure 2**).

Supervised, unsupervised, and logical filter image classifications were completed with ArcGIS Spatial Analyst (version 9.1, Environmental Systems Research Institute Inc.) using all four rasters (DEM, intensity, slope, and texture). The purpose of the classifications was to separate nine habitat classes from the four raster layers: water, mudflat–sandflat, vegetated mudflat, sand, mixed, cobble, patchy vegetation, thick vegetation, and trees–shrubs. Supervised and unsupervised classifications are standard methods for classifying imagery (Jensen, 2005), and therefore both methods were used to determine an optimal method for classifying lidar data. The logical filter classification procedure was developed as an alternative method for classifying imagery compared to the standard classification methods. Habitat class signatures were created using the training sites collected on Johnston's Pond, and a supervised classification was completed using a maximum likelihood algorithm (see **Figure 3**). To complete the unsupervised classification, the natural clustering of all four raster bands for nine classes was determined using the isodata clustering algorithm as described within Spatial Analyst (ESRI, 2005). The result of the clustering algorithm was used in a maximum likelihood algorithm to complete the unsupervised classification (see **Figure 3**). The Spatial Analyst raster calculator was used to develop a logical filter image classification (see **Figure 4**). The filter involved a preliminary classification that used the range of values between the minimum and maximum cell values extracted from the training sites of all four rasters.

These values were adjusted to create a more refined classification for each habitat class. Many beach classes had overlapping values within all four raster layers, making it difficult to classify some areas. If habitat classes overlapped,

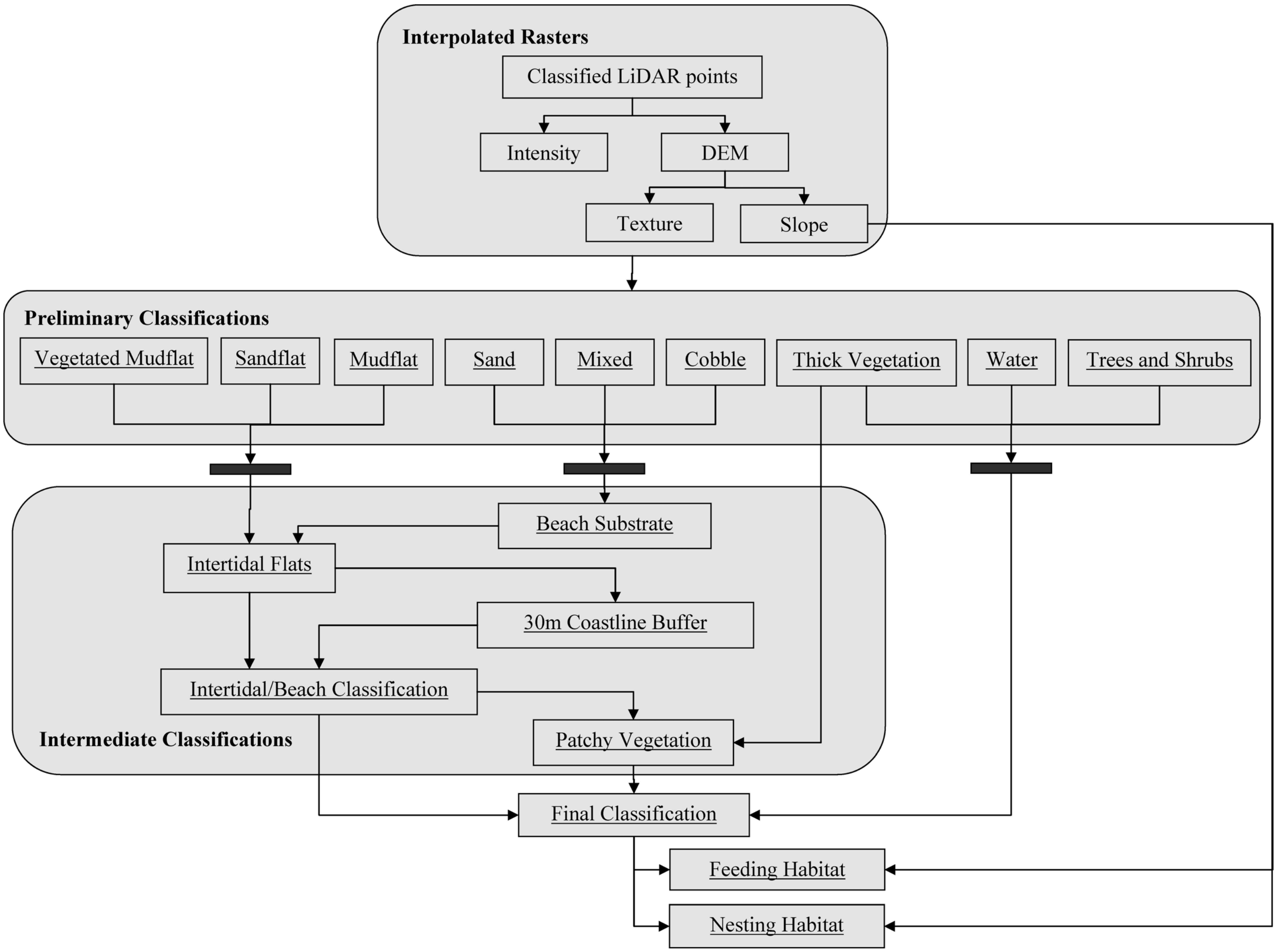

Figure 4. Illustration of the logical filter classification workflow. Pixel value ranges for the four input rasters were obtained from the training sites. The pixel ranges were then used to create preliminary classifications for all nine classes. Beach substrate and intertidal flats were identified through merging various classes using logical statements (see **Table 1**). From the intertidal flats output, pixels classified as vegetated mudflat that fell within 30 m of the coastline were classified as mudflat–sandflat. The newly classified mudflat–sandflat and intertidal flats outputs were merged to create the intertidal–beach classification. Patchy vegetation was determined if thick vegetation overlapped sand, mixed, or cobble. The remaining classes along with the intertidal–beach and patchy vegetation classifications were merged together to create the final classification. From the final classification, specific slopes and classes were used to identify critical feeding and nesting habitats (see **Table 2**).

then classes were arranged hierarchically or a new class was created (see **Table 1**). In some cases a proximity filter was used to classify conflicting habitat classes. For example, vegetated mudflat was classified in intertidal areas along the coastline that should have been classified as mudflat–sandflat. To solve this problem, any pixels classified as vegetated mudflat within 30 m of the coastline were classified as mudflat–sandflat.

Another type of logical filter classification was performed to identify important feeding and nesting habitat for piping plover. Environment Canada (2006) identified gently sloping beach habitat as a key habitat attribute. Unpublished research has shown that preferred habitat exhibited a beach slope of 3° (D.L. Amirault-Langlais and A.W. Boyne, personal communication). Furthermore, habitats such as mixed substrate, sand, and patchy vegetation have been identified as important nesting features (Environment Canada, 2006; Stewart, 2004; Flemming et al., 1992). Using the slope raster and logical filter classification, a new classification was completed to identify nesting habitat. The same method was also used for identifying feeding habitat, with feeding occurring primarily on sand, algal flats, and mudflats (Loegering and Fraser, 1995; Goossen et al., 2002; Stewart, 2004). The logical statements for these classifications are shown in **Table 2**.

To validate the three different classifications, the 78 GPS points collected in the Johnston's Pond study area were manually classified into one of the eight defined areas of interest based on the actual ground characteristics observed in

 © 2007 CASI

Table 1. Logical and hierarchical statements used in the logical filter for the intermediate and final classifications of Johnston's Pond.

Classification	Logical statement
Beach substrate	If mixed substrate overlaps sand and cobble, then classify as mixed
	If sand overlaps cobble, then classify as sand
Intertidal flats	If beach substrate overlaps mudflat, vegetated mudflat, or sandflat, then keep beach substrate classification
	If mudflat overlaps vegetated mudflat and sandflat, then classify as mudflat
	If vegetated mudflat overlaps sandflat, then classify as mudflat
	Merge mudflat and sandflat into one class (mudflat–sandflat)
Thirty metre (30 m) coastline buffer	If vegetated mudflat (from intertidal flats output) is within 30 m of the coastline, then classify as mudflat–sandflat
Intertidal–beach classification	Merge 30 m coastline buffer output with intertidal flats output
Patchy vegetation	If thick vegetation overlaps sand, mixed, or cobble, then classify as patchy vegetation
Final classification	Merge trees–shrubs over patchy vegetation over thick vegetation over water over intertidal–beach classification

Table 2. Logical statements used to classify critical piping plover nesting and feeding habitats.

Piping plover habitat classification	Logical statement
Critical feeding	If slope is less than or equal to 3.0° and beach habitat is classified as mudflat–sandflat or sand, then classify as feeding habitat
Critical nesting	If slope is less than or equal to 3.0° and beach habitat is classified as sand, mixed, or patchy vegetation, then classify as nesting habitat

the field. Furthermore, each point was taken in a homogeneous area of at least 2 m in diameter to be compared with the 1–2 m classified pixels. Using these GPS points, the classification values from the corresponding pixel locations were extracted in ArcMap and a comparison was completed in Microsoft Excel 2003 (Microsoft Corporation). If the classified GPS points matched the corresponding pixel classifications, then the classified pixel was considered to be correctly classified. Conversely, classified pixels that did not meet the corresponding GPS points were considered to be incorrectly classified.

Results

Each classified image was examined for accuracy using the ground validation points and training sites. The percentage of pixels correctly classified by the unsupervised, supervised, and logical filter classifications when compared with the training sites and validation points is shown in **Tables 3** and **4**, respectively.

Lidar validation

The results of the lidar validation collected on the same day as the survey flight demonstrate that the ALTM sensor was operating within the manufacturer-specified tolerance of 0.15 m for elevation and 1 m (1/2000 of the flying height) in the horizontal. A summary of the validation results for all 18 flight lines is provided in **Table 5**.

Unsupervised classification versus training sites

The unsupervised classification produced the most inaccurate classification when compared with the training sites. The mixed class overlapped with patchy vegetation and trees–shrubs and therefore was not classified. Cobble and thick vegetation were poorly classified, with less than 60% of the pixels being correctly separated. Conflict occurred between cobble and trees–shrubs, with 39% of the pixels being classified as trees–shrubs. Thick vegetation conflicted with patchy vegetation, resulting in 72% of the pixels being separated as patchy vegetation. However, mudflat, vegetated mudflat, sand, patchy vegetation, and trees–shrubs were all correctly classified above 80%.

Unsupervised classification versus validation points

Examining the validation point values compared with the unsupervised classification, it was found that 69% of the mudflat class was correctly classified, with the majority of the incorrectly classified areas occurring as sandy areas (some incorrectly classified data also occurred in vegetated mudflat and water areas). The highest percentage of correctly classified pixels occurred in the sand class at 80%, with 20% misclassified as thick vegetation. The remaining classes were poorly classified, with only 63% or less of the points being correctly classified. Mixed substrate and patchy vegetation could not be separated using the unsupervised classification, and therefore the patchy vegetation class was chosen to

Table 3. Percentage of classified pixels and total number of pixels for each classification method versus the training site values.

	Percentage of classified pixels within each training site									No. of Pixels		
	Water	Mudflat	Vegetated mudflat	Sand	Mixed	Cobble	Patchy vegetation	Thick vegetation	Trees–shrubs	Incorrect	Correct	Total
Supervised												
Mudflat	0	99	0	0	0	0	0	0	0	9	1718	1727
Vegetated mudflat	0	0	100	0	0	0	0	0	0	4	1672	1676
Sand	0	0	0	98	2	0	0	0	0	12	704	716
Mixed	0	0	0	7	84	1	7	0	0	61	329	390
Cobble–bedrock	0	0	0	0	2	96	0	0	1	83	2100	2183
Patchy dune vegetation	0	0	0	0	12	0	68	20	0	185	395	580
Thick dune vegetation	0	0	0	0	0	0	24	76	0	265	823	1088
Trees–shrubs	0	0	0	0	0	0	0	0	100	0	555	555
Total										619	8296	8915
Unsupervised												
Mudflat	0	98	0	2	0	0	0	0	0	32	1695	1727
Vegetated mudflat	0	0	86	13	0	0	0	1	0	268	1408	1676
Sand	0	0	0	100	0	0	0	0	0	1	715	716
Mixed	0	0	0	9	0	1	56	0	33	390	0	390
Cobble–bedrock	0	0	0	2	0	58	0	1	39	929	1264	2193
Patchy dune vegetation	0	0	0	3	0	0	86	11	0	82	498	580
Thick dune vegetation	0	0	0	0	0	0	72	27	0	792	296	1088
Trees–shrubs	0	0	0	0	0	0	0	3	97	19	536	555
Total										2513	6412	8925
Logical filter												
Mudflat	0	100	0	0	0	0	0	0	0	0	1727	1727
Vegetated mudflat	0	1	99	0	0	0	0	0	0	20	1641	1661
Sand	0	0	0	96	3	1	0	0	0	30	685	715
Mixed	0	0	0	7	75	6	13	0	0	98	292	390
Cobble–bedrock	0	0	0	0	1	97	0	1	0	62	2122	2184
Patchy dune vegetation	0	0	0	0	10	0	28	61	0	416	164	580
Thick dune vegetation	0	0	0	0	0	0	1	99	0	10	1078	1088
Trees–shrubs	0	0	0	0	0	0	0	0	100	0	551	551
Total										636	8260	8896

© 2007 CASI

Table 4. Percentage of classified pixels and total number of pixels for each classification method versus the validation points values.

	Percentage of classified pixels compared with validation points within each class									No. of pixels		
	Water	Mudflat	Vegetated mudflat	Sand	Mixed	Cobble	Patchy vegetation	Thick vegetation	Trees–shrubs	Incorrect	Correct	Total
Supervised												
Mudflat	38	38	19	6	0	0	0	0	0	10	6	16
Vegetated mudflat	5	5	84	0	0	5	0	0	0	3	16	19
Sand	0	0	0	80	0	0	20	0	0	1	4	5
Mixed	0	0	0	25	50	25	0	0	0	2	2	4
Cobble–bedrock	0	8	0	8	8	67	8	0	0	4	8	12
Patchy dune vegetation	0	0	0	13	0	0	63	25	0	3	5	8
Thick dune vegetation	0	0	0	0	13	0	50	38	0	5	3	8
Trees–shrubs	0	0	0	0	0	0	17	0	83	1	5	6
Total										29	49	78
Unsupervised												
Mudflat	6	69	6	19	0	0	0	0	0	5	11	16
Vegetated mudflat	0	26	47	26	0	0	0	0	0	10	9	19
Sand	0	0	0	80	0	0	0	20	0	1	4	5
Mixed	0	0	0	75	0	0	25	0	0	4	0	4
Cobble–bedrock	0	8	0	8	0	58	8	0	17	5	7	12
Patchy dune vegetation	0	0	38	0	0	0	25	38	0	6	2	8
Thick dune vegetation	0	0	25	13	0	0	0	63	0	3	5	8
Trees–shrubs	0	0	0	0	0	0	33	33	33	4	2	6
Total										38	40	78
Logical filter												
Mudflat	13	88	0	0	0	0	0	0	0	2	14	16
Vegetated mudflat	0	26	63	5	0	0	0	5	0	7	12	19
Sand	0	0	0	80	0	0	20	0	0	1	4	5
Mixed	0	0	0	25	75	0	0	0	0	1	3	4
Cobble–bedrock	0	8	0	0	8	83	0	0	0	4	8	12
Patchy dune vegetation	0	0	13	0	0	0	38	50	0	3	5	8
Thick dune vegetation	0	0	0	0	0	13	0	88	0	1	7	8
Trees–shrubs	0	0	0	0	0	0	0	17	83	1	5	6
Total										20	58	78

© 2007 CASI

Table 5. Lidar vertical and horizontal validation statistics for 18 flight lines.

Offset statistic	Elevation (*Z*)	Along-track flight direction (*X*)	Cross-track flight direction (*Y*)
Min. (M)	–0.28	–0.09	–0.83
Max. (M)	0.60	0.79	0.85
RMSE (M)	0.14	0.40	0.32
Avg. (M)	–0.09	0.35	–0.15
No. of samples	1424 points	12 edge crossings	508 edge crossings

Note: RMSE, root mean square error.

represent these overlapping areas, since more correctly classified pixels fell within the patchy vegetation class.

Supervised classification versus training sites

As expected, the supervised classification produced a high-quality classification when compared to the training sites. All classes except for patchy vegetation and thick vegetation showed good separability, with over 80% of the pixels being correctly classified. Not surprisingly, some conflict occurred between thick vegetation and patchy vegetation, 20% of pixels were misclassified as thick vegetation within the patchy vegetation training site, and 24% of the pixels were classified as patchy vegetation within the patchy vegetation training site.

Supervised classification versus validation points

The supervised classification was more effective at classifying beach habitat. Based on a priori knowledge of the area, the classification was suitable for classifying vegetated mudflat, sand, cobble, and patchy vegetation. Compared with the validation points, the vegetated mudflat class had the highest number of correctly classified pixels (84%) when judged against the other two classification methods. The supervised classification matched the results of the logical filter classification by accurately classifying sand (80%) and trees–shrubs (83%). Lower quality classifications occurred for the cobble–bedrock and patchy vegetation classes at 67% and 63%, respectively. Poor classifications (less than 50% correctly classified pixels) were found within the mudflat, thick vegetation, and mixed classes.

Logical filter classification versus training sites

When compared to the training sites, the logical filter classification produced a very good classification. All classes were above 90% except for mixed substrate and patchy vegetation. Mixed substrate was misclassified as patchy vegetation, cobble, and sand, resulting in only 75% of the pixels being correctly classified. Not surprisingly, patchy vegetation was mostly misclassified as thick vegetation, with a small portion misclassified as mixed substrate. This resulted in only 28% of the pixels within the patchy vegetation training site being correctly classified.

Logical filter classification versus validation points

The logical filter classification produced the best results out of the three classification methods (see **Figure 5**). Mudflat, sand, cobble, thick vegetation, and trees–shrubs all were validated, with 80% or more of the pixels correctly classified. The mixed class had a slightly lower percentage of 75%, and vegetated mudflat and patchy vegetation were less than 70%.

Classification of nesting and feeding habitat

Figure 6 shows identified nesting and feeding habitat based on optimal slope (<3°) and the logical filter classification. Based on a priori knowledge of the area and field observations of where piping plover nest and feed, this method of classifying habitat was generally accurate. Piping plovers have been observed in the mudflats and sandy areas immediately adjacent to nesting sites, which are accurately identified in **Figure 6**. However, the identified nesting and feeding areas in the northeast end of the map are less likely to be used by plovers because they are not adjacent to nesting sites. Upon closer examination of the 2005 nesting sites, it was found that the nests were not located within the classified nesting areas, although nesting habitat was identified within a few metres of the nest locations. The reason for this was that the chosen logic for an optimal slope value of 3° in the slope-based classification resulted in any areas with a steeper slope not being classified as nesting habitat. Both nests occurred on steeper slopes (approximately 7°) in 2005, and the nesting sites were correctly classified as nesting habitat when the slope parameter was increased to 7°. **Figure 6** also shows how the main nesting and feeding areas are closely related with the delineated critical habitat boundary. This exercise illustrates how renewed or updated understanding of a landscape or habitat process can be incorporated within a logical filter classification to maintain accurate results.

Discussion

Laser pulse intensity was found to be the most important layer of information when classifying coastal habitat using lidar data. Elevation played an important role in separating certain classes such as mudflats from the dune areas, which were classed as thick vegetation and patchy vegetation. Dunes are at elevations higher than sea level, whereas the mudflats are very close to sea level, and thus the classification could easily separate the difference between these classes. Slope was found to play a role in separating features such as cobble beach from mudflats, since exposed coastal beaches are generally sloped

 © 2007 CASI

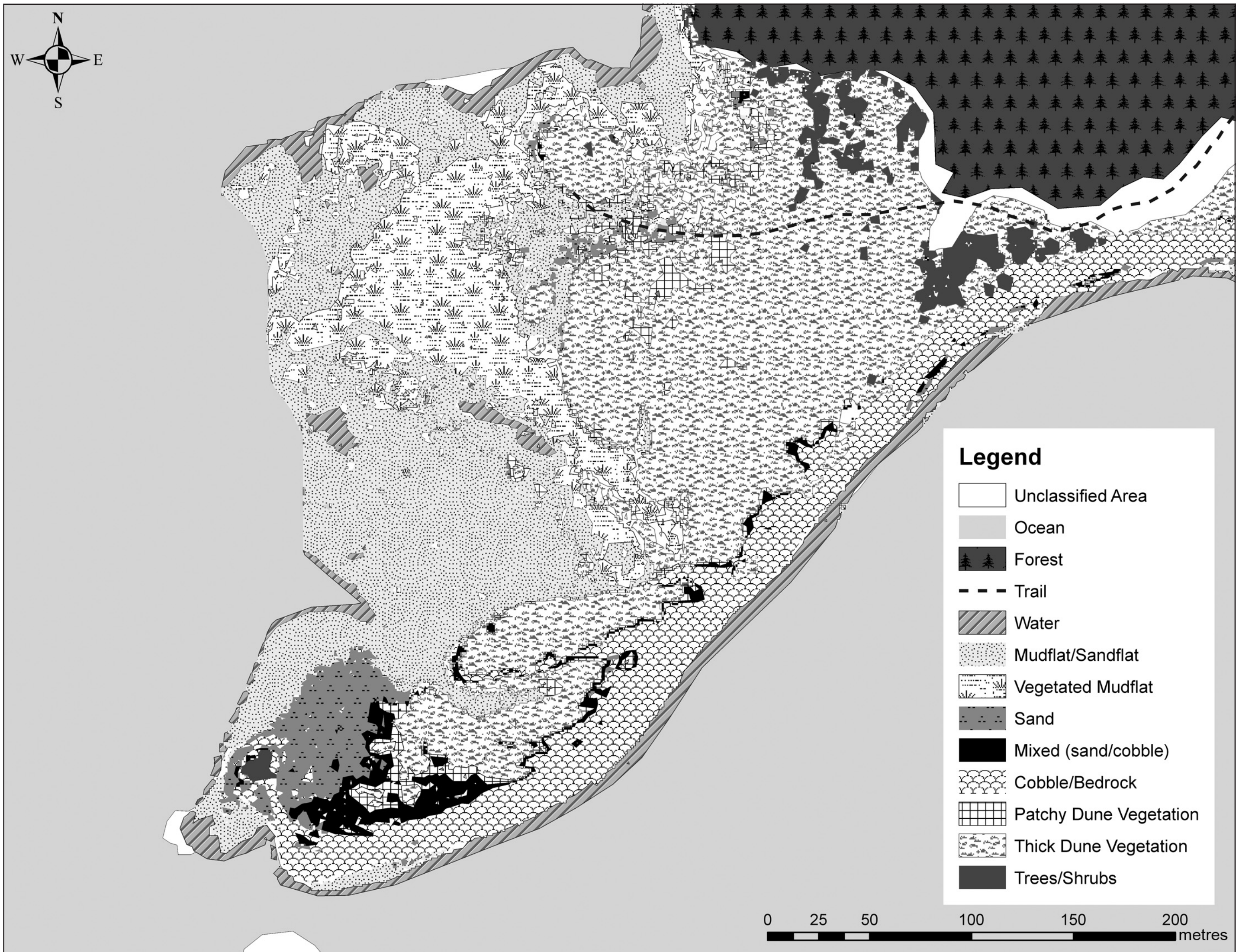

Figure 5. Logical filter classification of coastal habitat on Johnston's Pond Beach.

owing to wave action compared with the protected salt-marsh–mudflat areas, which are extremely flat.

With the exception of areas of tall trees and shrubs, texture did not seem to have a strong influence on the classifications, as originally anticipated. Texture was only minimally useful to separate vegetated areas. The majority of marram grass covering the dune systems was around 0.30–0.50 m in height. Laser pulse returns in areas of thick marram grass could have reflected off the surface of the grass without any ground returns or more likely may have penetrated through the grass because of the minimal planar surface area exposed by the stalks (e.g., Hopkinson et al., 2005; Töyra et al., 2003). In this case, areas would be classed as having an artificially low surface height range (texture), which would produce a textural result similar to that of sand or mudflat areas.

The water, mudflat, vegetated mudflat, and sand classifications were found to conflict with one another. These landscape features were the most difficult classes to separate using the logical filter classification. Upon close examination, these areas were found to be nearly identical in their slope, texture, and elevation values, with much overlap. The intensity raster values were the most important data separating these classes; however, these values also overlapped between classes. Based on photographs and field ground-truthing, the overlapping mudflat and vegetated mudflat areas were found to be supersaturated with water at the time of lidar capture. Lidar intensity is determined in the near-infrared portion of the electromagnetic spectrum and thus will be absorbed by water or saturated substrates. Since the lidar survey was flown in the fall, much of the grass and vegetation covering the mudflat had died or was losing its vigor. Laser pulses were most likely not reflecting strongly off the dead vegetation but rather were hitting the saturated soil, which resulted in an intensity return similar to that of mudflat. Sandy areas were most likely misclassified, since any sandy areas that were damp from rain or ocean spray may have produced intensity values similar to those of saturated mudflat or vegetated mudflat.

© 2007 CASI

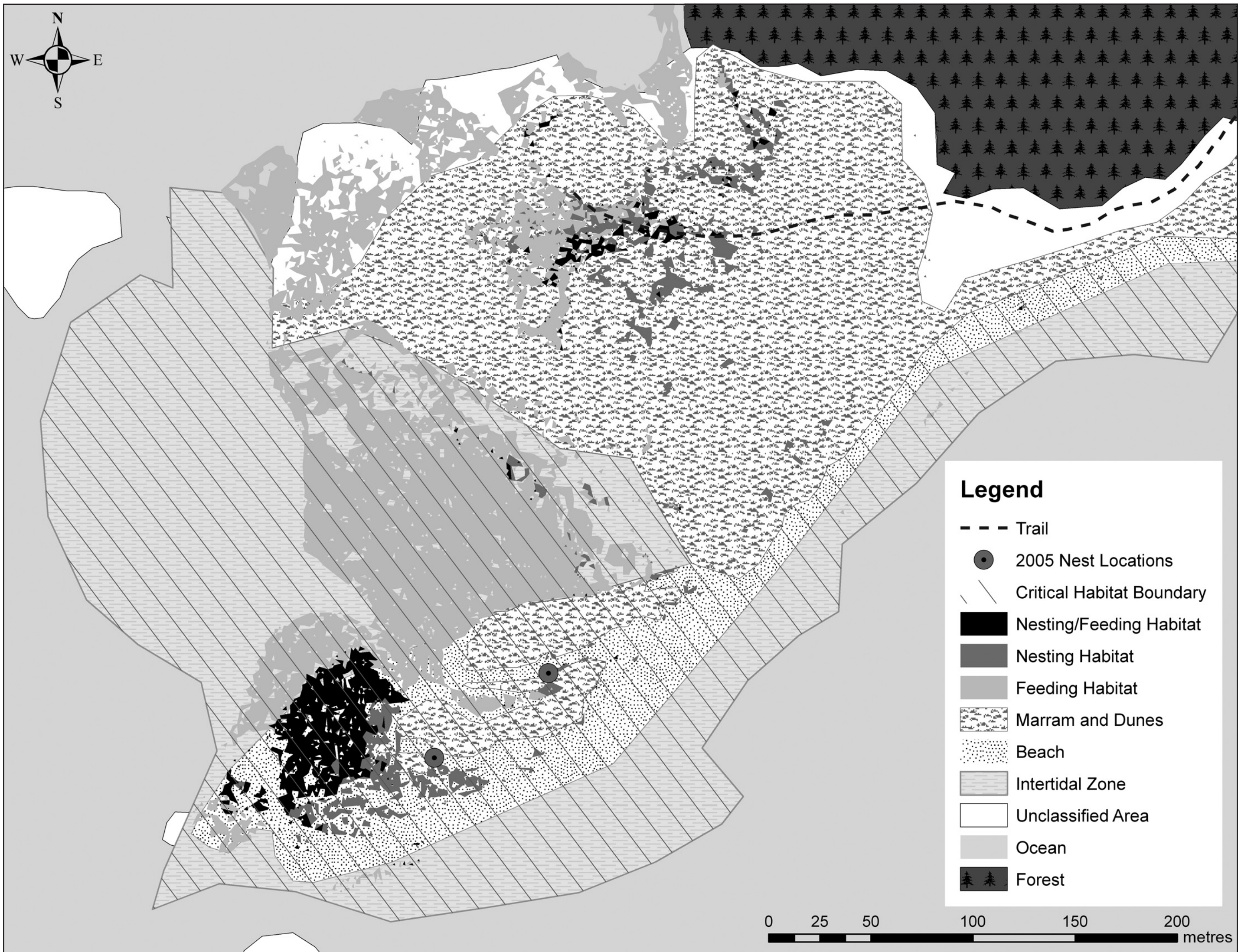

Figure 6. Logical filter classification showing nesting and feeding habitat for piping plover on Johnston's Pond Beach. The map shows nesting locations in 2005 and delineated critical habitat boundaries in relation to the classified habitat.

Mixed substrate was misclassified as either sand or cobble in some of the classifications. In addition, cobble seemed to be misclassified as sand or mixed because they most likely have similar intensity values. Patchy vegetation had the poorest separability, with many pixels being misclassified as thick vegetation. The patchy vegetation class was difficult to categorize, since it can be comprised of patches of vegetation that may resemble thick vegetation, and the areas between the vegetation patches may be classified as sand, mixed, or cobble substrate.

As expected, the logical filter classification generally produced the best results. However, there was one notable exception in that the supervised classification produced better results for classifying vegetated mudflat.

Although the logical filter was effective on Johnston's Pond Beach, it is unlikely that this logical classification model could be applied in its current form to other beaches or even the same beach at a different time and attain comparable results. Training sites and validation points should be collected on all beaches around the same time as the airborne lidar collection. Using the logical filter methodology with site-specific training sites and validation points will ensure quality results.

Conclusions

Lidar offers a means of using combined spectral and elevation data to classify coastal habitat. This study has demonstrated that intensity and elevation data can be used effectively to classify coastal habitat using a logical filter classification model. However, completely accurate differentiations between complicated and overlapping feature classes such as mixed substrate and patchy vegetation versus thick vegetation may not be possible. To increase the chance of

© 2007 CASI

successful classifications over coastal habitats, it is recommended that lidar data be acquired in the summer months when vegetation is vigorous for better separability between mudflat–sandflat and vegetated mudflat land-cover classes. Furthermore, flying in dry conditions coincident with or immediately following lowest low tide would be optimal to reduce the effects of overlapping intensity values from saturated sand and mudflats. Classifications would likely be improved by the addition of further high-resolution remote sensing data layers such as luminance derived from true colour digital orthorectified photographs or lidar systems with an optical sensor.

Using a logical filter classifier, it is possible to isolate important physical habitat characteristics that are elevation and substrate dependent, such as piping plover nesting and feeding habitat. An advantage of such an approach over traditional supervised and unsupervised techniques might be that as updated data or renewed understanding of coastal habitat processes becomes available, this new understanding can readily be applied to the physically based logical classification model, without the need to retrain the entire classification.

Lidar is being increasingly applied in coastal and riparian zones for flood impact assessments all around the world (Heinzer et al., 2000; Gutierrez et al., 2001; Brock et al., 2002; FEMA, 2003; Lane et al., 2003; Webster et al., 2003; 2004; 2005; 2006; Rath and Pasche, 2004; Haile, 2005; Balmforth and Dibben, 2006; Webster and Forbes, 2006). Consequently, a large volume of lidar data is accumulating in these types of environments. Coastal flooding is an important and growing social concern and constitutes enormous justification for the collection of costly lidar data for flood risk mapping. However, flood risk mapping is only one application in coastal areas. There is a growing body of literature showcasing the application of lidar in coastal and riparian environments for a wide variety of applications such as monitoring beach change (Gibeaut et al., 2001; Adams and Chandler, 2002; Revell et al., 2002; Woolard and Colby, 2002; Sallenger et al., 2003; Mitasova et al., 2003) and coastal–riparian mapping (Brock et al., 2001; Populus et al., 2001; Weber et al., 2005; Xiaojun, 2005). Through these additional applications, the value of coastal zone lidar datasets increases, and the cost of obtaining them is further justified. Although coastal habitat mapping is not likely a profitable application on its own, there is a genuine need to develop these types of applications so that we can derive useful “value-added” products. We can then maximize the use of coastal lidar datasets and benefits to our coastal ecosystems.

Acknowledgements

Special thanks to Richard Brunt and Chris McCarthy from Kejimkujik National Park and National Historic Site for their support. Thank you to the Applied Geomatics Research Group for being the centre and driving force for this research, especially Bob Maher, Laura Chasmer, Tim Webster, Darren Billard, and Trevor Milne. Tristan Goulden and Chris Beasy are acknowledged for assistance with collection of the GPS runway validation data. Thank you to the Canadian Wildlife Service for their support. This project was funded through the Environment Canada Science Horizons Youth Internship Program.

References

Adams, J., and Chandler, J. 2002. Evaluation of lidar and medium scale photogrammetry for detecting soft-cliff coastal change. *The Photogrammetric Record*, Vol. 17, No. 99, pp. 405–418(14).

Balmforth, D.J., and Dibben, P.A. 2006. Modelling tool for assessing flood risk. *Water Practice & Technology*, Vol. 1, No. 1, p. 8.

Baltsavias, E.P. 1999. A comparison between photogrammetry and laser scanning. *Journal of Photogrammetry and Remote Sensing*, Vol. 54, pp. 83–94.

Beasy, C., Hopkinson, C.H., and Webster, T. 2005. Classification of nearshore materials on the Bay of Fundy coast using LiDAR intensity data. In *Proceedings of the 26th Canadian Symposium on Remote Sensing*, 14–16 June 2005, Wolfville, N.S. CD-ROM. Canadian Aeronautics and Space Institute (CASI), Ottawa, Ont. Paper 11.

Boates, J.S., Austin-Smith, P., Dickie, G., Williams, R., and Sam, D. 1994. *Nova Scotia piping plover atlas*. Nova Scotia Department of Natural Resources, Kentville, N.S. 86 pp.

Brennan, R., and Webster, T.L. 2006. Object-oriented land cover classification of lidar-derived surfaces. *Canadian Journal of Remote Sensing*, Vol. 32, No. 2, pp. 162–172.

Brock, J.C., Sellenger, A.H., Krabill, W.B., Wright, C.W., and Swift, R.N. 2001. Recognition of fiducial surfaces in lidar surveys of coastal topography. *Photogrammetric Engineering & Remote Sensing*, Vol. 67, No. 11, pp. 1245–1258.

Brock, J.C., Wright, C.W., Sallenger, A.H., Krabill, W.B., and Swift, R.N. 2002. Basis and methods of NASA airborne topographic mapper LIDAR surveys for coastal studies. *Journal of Coastal Research*, Vol. 18, pp. 1–13.

Burger, J. 1987. Physical and social determinants of nest-site selection in Piping Plover in New Jersey. *The Condor*, Vol. 89, pp. 811–818.

Burtch, R. 2002. LIDAR principles and applications. In *Proceedings of the IMAGIN Conference 2002: Geography on the Move*, 29 April – 1 May 2002, Traverse City, Mich. IMAGIN, Southfield, Mich. p. 13.

Charaniya, A.P., Manduchi, R., and Lodha, S.K. 2004. *Supervised parametric classification of aerial LiDAR data* [online]. Available from www.cse.ucsc.edu/~manduchi/papers/Amin3D.pdf [cited September 2005].

Department of Fisheries and Oceans Canada. 1996. *Module 6: sandy beaches and dunes. A guide to the coastal zone of Atlantic Canada*. Department of Fisheries and Oceans Canada, Moncton, N.B.

Environment Canada. 2006. *Recovery strategy for piping plovers (Charadrius melodus melodus) in Canada [Proposed]*. Environment Canada, Ottawa, Ont. Species at Risk Act Recovery Strategy Series. 46 pp.

ESRI. 2005. *Spatial analyst extension*. ArcGIS Version 9.1. ArcMap Help. CD-ROM. Environment Systems Research Institute (ESRI), Redlands, Calif.

FEMA. 2003. Appendix A: guidance for aerial mapping and surveying. In *Guidelines and specifications for flood hazard mapping partners* [online].

© 2007 CASI

Federal Emergency Management Agency (FEMA), Washington, D.C. Available from www.fema.gov/fhm/dl_cgs.shtm [cited October 2007].

Flemming, S.P., Chiasson, R.D., and Austin-Smith, P.J. 1992. Piping Plover nest site selection in New Brunswick and Nova Scotia. *Journal of Wildlife Management*, Vol. 56, pp. 578–583.

French, J.R. 2003. Airborne LiDAR in support of geomorphological and hydraulic modeling. *Earth Surface Processes and Landforms*, Vol. 28, pp. 321–335.

Gibeaut, J.C., Hepner, T., Waldinger, R., Andrews, J., Gutierrez, R., Tremblay, T.A., Smyth, R., and Xu, L. 2001. *Changes in Gulf shoreline position, Mustang and North Padre islands, Texas*. A report of the Texas Coastal Coordination Council pursuant to National Oceanic and Atmospheric Administration award NA97OZ0179 [online]. Bureau of Economic Geology, The University of Texas at Austin, Austin, Tex. Available from www.beg.utexas.edu/coastal/presentations_reports/Mustangfinalrpt.pdf [cited September 2005]. 30 pp.

Goossen, J.P., Amirault, D.L., Arndt, J., Bjorge, R., Boates, S., Brazil, J., Brechtel, S., Chiasson, R., Corbett, G.N., Curley, R., Elderkin, M., Flemming, S.P., Harrris, W., Heyens, L., Hjertaas, D., Huot, M., Johnson, B., Jones, R., Koonz, W., Laporte, P., McAskill, D., Morrison, R.I.G., Richard, S., Shaffer, F., Stewart, C., Swanson, L., and Wiltse, E. 2002. *National Recovery Plan for the Piping Plover (Charadrius melodus)*. National Recovery Plan 22. Recovery of Nationally Endangered Wildlife. Canadian Wildlife Service, Environment Canada, Ottawa. 47 pp.

Gutierrez, R., Gibeaut, J.C., Smyth, R.C., Helpner, T.L., and Andrews, J.R. 2001. Precise airborne LiDAR surveying for coastal research and geohazards applications. *International Archives of Photogrammetry and Remote Sensing*, Vol. 35, No. 3, pp. 22–24.

Haig, S.M., and Elliott-Smith, E. 2004. Piping plover. In *The birds of North America online*. Edited by A. Poole. Cornell Laboratory of Ornithology, Ithaca, N.Y. Retrieved from the birds of North American online database [online]. Available from bna.birds.cornell.edu/BNA/account/Piping_Plover/ [cited September 2005].

Haile, A.T. 2005. *Integrating hydrodynamic models and high resolution DEM (LIDAR) for flood modelling*. M.Sc. thesis, International Institute for Geo-information Science and Earth Observation, Enschede, Netherlands.

Heinzer, T., Sehbat, M., Feinberg, B., and Kerper, D. 2000. The use of GIS to manage LIDAR elevation data and facilitate integration with the MIKE21 2-D hydraulic model in a flood inundation decision support system. In *Proceedings of the 2000 ESRI Users' International Conference*, June 2000, San Diego, Calif. [online]. Available from gis.esri.com/library/userconf/proc00/professional/papers/PAP675/p675.htm [cited October 2007].

Hopkinson, C. 2007. The influence of flying altitude, beam divergence, and pulse repetition frequency on laser pulse return intensity and canopy frequency distribution. *Canadian Journal of Remote Sensing*, Vol. 33, No. 4, pp. 312–324.

Hopkinson, C., Chasmer, L.E., Sass, G., Creed, I.F., Sitar, M., Kalbfleisch, W., and Treitz, P. 2005. Vegetation class dependent errors in lidar ground elevation and canopy height estimates in a boreal wetland environment. *Canadian Journal of Remote Sensing*, Vol. 31, No. 2, pp. 191–206.

Jensen, J.R. 2005. *Introductory digital image processing: a remote sensing perspective*. Pearson Prentice Hall, Upper Saddle River, N.J. 526 pp.

Lane, S.N., James, T.D., Pritchard, H., and Saunders, M. 2003. Photogrammetric and laser altimetric reconstruction of water levels for extreme flood event analysis. *The Photogrammetric Record*, Vol. 18, No. 104, p. 293.

Leica Geosystems AG. 1999. *GPS surveying – system 500* [online]. Leica Geosystems AG, Heerbrugg, Switzerland. Available from www.leica-geosystems.com/corporate/en/support/lgs_page_catalog.htm?cid = 2703 [cited August 2007].

Loegering, J.P., and Fraser, J.D. 1995. Factors affecting Piping Plover chick survival in different brood-rearing habitats. *Journal of Wildlife Management*, Vol. 59, No. 4, pp. 646–655.

Mitasova, H., Bernstein, D., Drake, T.G., Harmon, R., and Miller, C.H. 2003. Spatio-temporal analysis of beach morphology using LIDAR, RTK-GPS and Open source GRASS GIS. In *Coastal Sediments 03: Proceedings of the Fifth International Conference on Coastal Sediments*, 18–23 May 2003, Clearwater Beach, Fla. CD-ROM. World Scientific Publishing Corp. and East Meets West Productions, Corpus Christi, Tex.

Morrison, R.I.G., Butler, R.W., Beyersbergen, G.W., Dickson, H.L., Bourget, A., Hicklin, P.W., Goossen, J.P., Ross, R.K., and Gratto-Trevor, C.L. 1995. *Potential western hemisphere shorebird reserve network sites for shorebirds in Canada*. 2nd ed. Canadian Wildlife Service, Environment Canada, Ottawa, Ont. Canadian Wildlife Service Technical Report Series 227. 104 pp.

Populus, J., Barreau, G., Fazilleau, J., Kerdreux, M., and L'Yavanc, J. 2001. Assessment of the Lidar topographic technique over a coastal area. In *CoastGIS 2001: Managing the Interfaces* [online], 18–20 June 2001, Halifax, N.S. Available from www.coastgis.org/01pdfs/populus.pdf [cited October 2007].

Rangeley, R., and Singh, R. 2000. *A framework for biological monitoring in marine protected areas: a proposal for the Musquash Estuary*. Conservation Council of New Brunswick, Fredericton, N.B. 18 pp.

Rath, S., and Pasche, E. 2004. Hydrodynamic floodplain modeling based on high-resolution LiDAR measurements. In *Proceedings of the 6th International Conference on Hydroinformatics*, 21–24 June 2004, Singapore [online]. Edited by S.-Y. Liong, K. Phoon, and V. Babovic. World Scientific Publishing Company, Singapore. Available from elbe.wb.tu-harburg.de/mitarbeiter/rath/rath_hic169_june2004_download-tuhh.pdf [cited October 2007]. pp. 486–493.

Revell, D.L., Komar, P.D., and Sallenger, A.H., Jr. 2002. An application of LIDAR to analyses of El Nino erosion in the Netarts Littoral Cell, Oregon. *Journal of Coastal Research*, Vol. 18, No. 4, pp. 792–801.

Sallenger, A.H., Jr., Krabill, W.B., Swift, R.N., Brock, J., List, J., Hansen, M., Holman, R.A., Manizade, S., Sontag, J., Meredith, A., Morgan, K., Yunkel, J.K., Frederick, E.B., and Stockdon, H. 2003. Evaluation of airborne topographic lidar for quantifying beach changes. *Journal of Coastal Research*, Vol. 19, No. 1, pp. 125–133.

Song, J.-H., Han, S.-H., Yu, K.Y., and Kim, Y.-I. 2002. Assessing the possibility of land-cover classification using Lidar intensity data. In *Photogrammetric Computer Vision: Proceedings of the ISPRS Commission III Symposium 2002*, 9–13 September 2002, Graz, Austria. [online] Available from www.isprs.org/commission3/proceedings/papers/paper128.pdf [cited September 2005]. Vol. XXXIV, Part B, pp. 259–262.

Stewart, J. 2004. *A multi-scale habitat suitability assessment for Piping Plover (Charadrius melodus melodus) in Prince Edward Island*. M.Sc. thesis, School for Resource and Environmental Studies, Dalhousie University, Halifax, N.S. 168 pp.

Töyrä, J., Pietroniro, A., Hopkinson, C., and Kalbfleisch, W. 2003. Assessment of airborne scanning laser altimetry (lidar) in a deltaic wetland environment. *Canadian Journal of Remote Sensing*, Vol. 29, No. 6, pp. 718–728.

US Fish and Wildlife Service. 1996. *Piping plover (Charadrius melodus) and Atlantic Coast population, revised recovery plan* [online]. US Fish and

 © 2007 CASI

Wildlife Service, Hadley, Mass. Available from ecos.fws.gov/docs/recovery_plans/1996/960502.pdf [cited September 2005]. pp. 258.

Weber, K.M., List, J.H., and Morgan, K.L.M. 2005. *An operational mean high water datum for determination of shoreline position from topographic lidar data*. US Geological Survey, Open-file Report 2005-1027.

Webster, T.L., and Forbes, D.L. 2006. Airborne laser altimetry for predictive modeling of coastal storm-surge flooding. In *Remote sensing of aquatic coastal ecosystem processes: science and management applications*. Edited by L.L. Richardson and E.F. LeDrew. Springer, New York. Chapt. 7, pp. 157–182.

Webster, T.L., Dickie, S., O'Reilly, C., Forbes, D.L., Parkes, G., Poole, D., and Quinn, R. 2003. Mapping storm-surge flood risk using a LIDAR-derived DEM. *Elevation (Supplement to Geospatial Solutions and GPS World)*, May 2003, pp. 4–9.

Webster, T.L., Forbes, D.L., Dickie, S., and Shreenan, R. 2004. Using topographic lidar to map flood risk from storm-surge events for Charlottetown, Prince Edward Island, Canada. *Canadian Journal of Remote Sensing*, Vol. 30, No. 1, pp. 64–76.

Webster, T., Christian, M., Sangster, C., and Kingston, D. 2005. High-resolution elevation and image data within the Bay of Fundy coastal zone, Nova Scotia, Canada. In *GIS for coastal zone management*. Edited by D. Bartlett and J. Smith. CRC Press, Danvers, Mass. pp. 195–218.

Webster, T.L., Forbes, D.L., MacKinnon, E., and Roberts, D. 2006. Flood-risk mapping for storm-surge events and sea-level rise using lidar of southeast New Brunswick. *Canadian Journal of Remote Sensing*, Vol. 32, No. 2, pp. 194–211.

Wehr, A., and Lohr, U. 1999. Airborne laser scanning – an introduction and overview. *Journal of Photogrammetry and Remote Sensing*, Vol. 54, pp. 68–82.

Woolard, J.W., and Colby, J.D. 2002. Spatial characterization, resolution, and volumetric change of coastal dunes using airborne LIDAR: Cape Hatteras, North Carolina. *Geomorphology*, Vol. 48, No. 1–3, pp. 269–287.

Xiaojun, Y. 2005. Use of LIDAR elevation data to construct a high resolution digital terrain model for an estuarine marsh area. *International Journal of Remote Sensing*, Vol. 26, No. 23, pp. 5163–5166(4).